tvst

Lacrimal Apparatus, Eyelids, Orbit

Development of Artefact-Free Imaging System for Accurate Meibomian Gland Reflectivity Assessment

Kasandra Swiderska[1], Caroline A. Blackie[2], Carole Maldonado-Codina[1], Martin Fergie[3], Philip B. Morgan[1], and Michael L. Read[1]

[1] Eurolens Research, Division of Pharmacy and Optometry, Faculty of Biology, Medicine and Health, The University of Manchester, Manchester, UK
[2] Johnson & Johnson Vision, Inc., Jacksonville, FL, USA
[3] Division of Informatics, Imaging and Data Sciences, Faculty of Biology, Medicine and Health, The University of Manchester, Manchester, UK

Correspondence: Kasandra Swiderska, Eurolens Research, The University of Manchester, Carys Bannister Building, Dover Street, Manchester, M13 9PL, UK.
e-mail: kasandra.swiderska@gmail.com

Received: September 20, 2022
Accepted: January 6, 2023
Published: February 7, 2023

Keywords: meibography; meibomian gland contrast; meibomian gland imaging; meibomian gland intensity; meibomian glands

Citation: Swiderska K, Blackie CA, Maldonado-Codina C, Fergie M, Morgan PB, Read ML. Development of artefact-free imaging system for accurate meibomian gland reflectivity assessment. Transl Vis Sci Technol. 2023;12(2):9, https://doi.org/10.1167/tvst.12.2.9

Purpose: To develop and evaluate a custom imaging system to provide high-resolution, wide depth-of-field, reflection-free, multispectral infrared (IR) imaging of the Meibomian glands.

Methods: Lower eyelids of 15 volunteers were everted to obtain multispectral images of the Meibomian glands with custom imaging setup. Photographs were captured at 10 different ISO settings (from underexposure to overexposure) and using nine IR imaging filters (ranging from 600 nm to 1000 nm in 50-nm steps). Meibomian gland contrast (simple and Michelson) was calculated for the images to choose an optimal wavelength for Meibomian gland imaging and to determine differences in contrast across individuals.

Results: The overall linear regression model showed a significant effect of wavelength on Meibomian gland contrast (Simple contrast: $F = 7.24$, $P < 0.0001$; Michelson contrast: $F = 7.19$, $P < 0.0001$). There was a significant negative correlation between Meibomian gland contrast and Meibomian gland depth for 750-nm IR filter ($\rho_s = -0.579$; $P = 0.026$).

Conclusions: Meibomian gland contrast varies across individuals and depends on Meibomian gland depth. IR filter of 750 nm is the optimal choice for Meibomian gland imaging because it provides images of greatest contrast.

Translational Relevance: This study adds to our understanding of Meibomian gland imaging. It has successfully demonstrated that Meibomian glands that are deeper in the tarsal plate require longer wavelengths for imaging.

Introduction

Meibography is a visualization technique that allows observations of morphological changes of the Meibomian glands - the sebaceous glands in the eyelids which are primarily responsible for producing the lipid layer of the tear film (meibum). Meibomian glands can appear as dark areas on a light background in the transillumination technique or as light areas on a dark background in the direct illumination technique. It is still unknown whether highlighted acinar areas show actual gland structure or rather, functional acini. In other words, it is uncertain whether the apparent absence of Meibomian glands during imaging (dropout) indicates Meibomian gland loss, altered or absent meibum, an accumulation of keratinized cells,[1,2] or indeed none of these phenomena.

Hwang et al.[3] have measured the spectral absorption profile for the Meibomian gland and other eyelid structures, including eyelid muscle and tarsal plate. They reported that lipid droplets present in meibocytes are the major cause of light scattering and decreased light transmission, suggesting that meibography detects active lipid synthesis in differentiating meibocytes.[3] A case report of a 19-year-old Asian

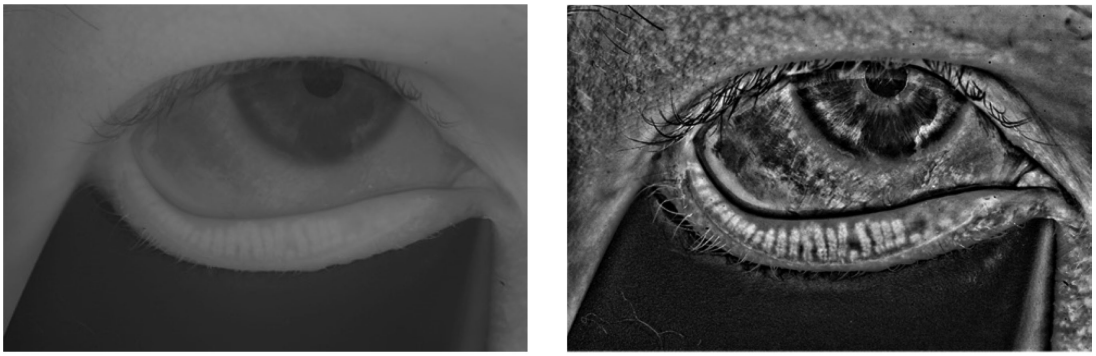

(a) (b)

Figure 1. An example of potential image enhancement (b) that could be applied to images captured with the proposed imaging setup (a) presented in the current study.

male patient treated with isotretinoin suggests that the reflectivity of Meibomian glands could be an indicator of gland function because reflectivity decreased during treatment and then increased after discontinuation.[4] This observation has been explained by the fact that isotretinoin shrinks human sebaceous glands, increases the presence of undifferentiated cells, and inhibits sebum production.[4–6] In addition, the authors noted that the length of the Meibomian glands remained fairly constant throughout.[4] Similar observations have been reported by Tanriverdi et al.,[7] who assessed the longitudinal changes in Meibomian glands in 88 patients receiving systemic isotretinoin treatment. The contrast of Meibomian glands decreased rapidly from the first month of treatment and continued to worsen until 6 months. Contrast gradually increased after the end of treatment; however, 12 months after the end of treatment, it remained below the baseline level. Interestingly, other Meibomian gland characteristics such as dropout, distortion, and shortening showed similar behavior. The reported results clinically support the earlier findings that systemic isotretinoin use suppresses meibum synthesis in Meibomian glands.[7] Singh et al.,[8] however, showed that the dark areas seen on meibography that correspond with Meibomian gland dropout have no residual glandular structure on histology, suggesting that Meibomian gland atrophy reflects the absence of glandular elements rather than altered lipid content.

Meibomian gland contrast and gland visibility have been used as indicators of Meibomian gland health on a number of occasions.[4,9–11] There have been many ways of measuring gray intensity levels of meibography images including both intragland and intergland Michelson contrast, kurtosis, and skewness of histograms of the gland regions, or relative energy, entropy, and standard deviation irregularity of the selected pixels.[9,10]

The experiment reported here sought to evaluate a custom imaging system that has been developed to provide high-resolution, wide depth-of-field, reflection-free, multispectral infrared (IR) imaging of the Meibomian glands. Commercially available clinical instruments used for Meibomian gland imaging either do not typically allow access to the raw captured image and present only a highly processed image or provide images that are affected by specular reflections. The images captured with the proposed setup are unprocessed, in contrast with other commercially available devices; however, if needed, image enhancement may be applied to analyze other Meibomian gland structure metrics (Fig. 1). In addition, these instruments typically capture clinical images in a highly inconsistent manner, with camera settings such as exposure and gain automatically altered in an attempt to optimize the clinical image. Figure 2 shows examples of 10 consecutive images captured with our imaging setup and with two most popular commercial instruments used for meibography, namely, the Keratograph 5M (OCULUS, Wetzlar, Germany) and the LipiView II (Johnson & Johnson Vision, Irvine, CA). These factors mean that potentially useful clinical metrics, such as accurate measurement of Meibomian gland reflectivity and intensity, are compromised. Furthermore, these commercially available instruments typically operate at a single IR wavelength that is assumed to fit all. We hypothesize that different individuals may require different IR imaging wavelengths to optimize clinical Meibomian gland imaging. Our work, therefore, aimed to investigate how Meibomian gland imaging is influenced by changing wavelength and camera exposure settings. This project will allow optimal camera settings to be defined for future clinical studies and provide

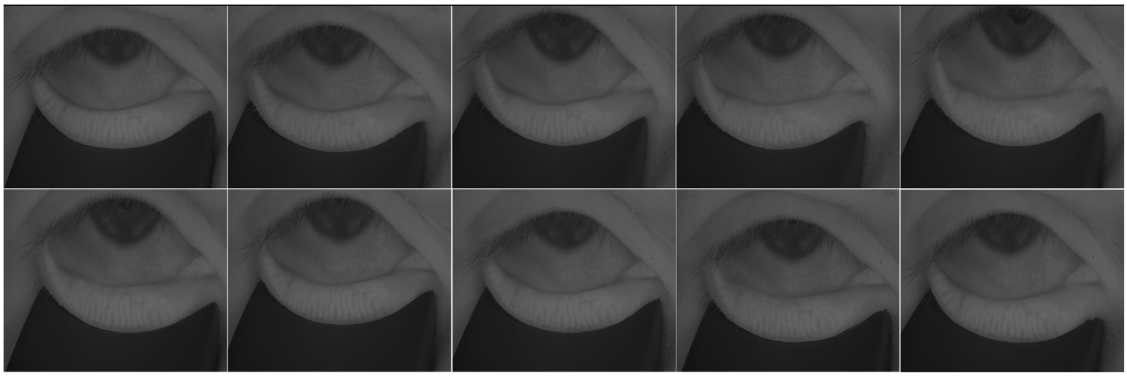

(a) Custom imaging setup

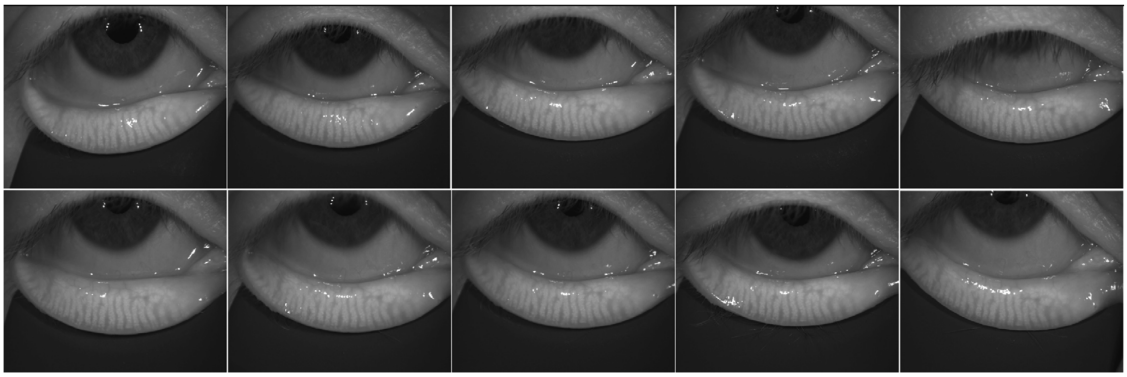

(b) Keratograph 5M

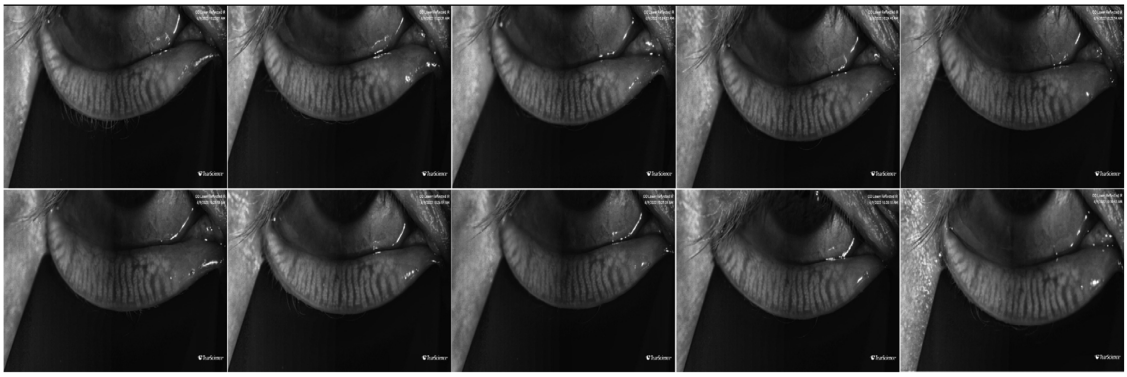

(c) LipiView II

Figure 2. Examples of 10 consecutive photographs captured for the same eyelid with 3 different imaging devices. Each image captured at separate eyelid eversion. Photographs captured with a custom imaging setup presented in this article (a) are high resolution, wide depth of field, and reflection free. Keratograph 5M provides raw images with many specular reflections dependent on eyelid eversion (b). LipiView II provides only processed images with enhanced contrast which are not consistent with respect to illumination (c).

initial clinical data relating to imaging wavelength and Meibomian gland reflectivity to allow power analysis for future clinical studies.

Methods

Participants

This study was approved by the University Research Ethics Committee of The University of Manchester before participant recruitment. All procedures adhered to the tenets of the Declaration of Helsinki and all participants provided written informed consent before enrolment. Study participants attended a single study visit lasting approximately 60 minutes.

Participants were at least 18 years of age, were willing and able to sign a Statement of Informed Consent and follow the protocol, and agreed not to participate in other clinical research for the duration of this study. Participants were not eligible to take part in the study if they had history of any ocular

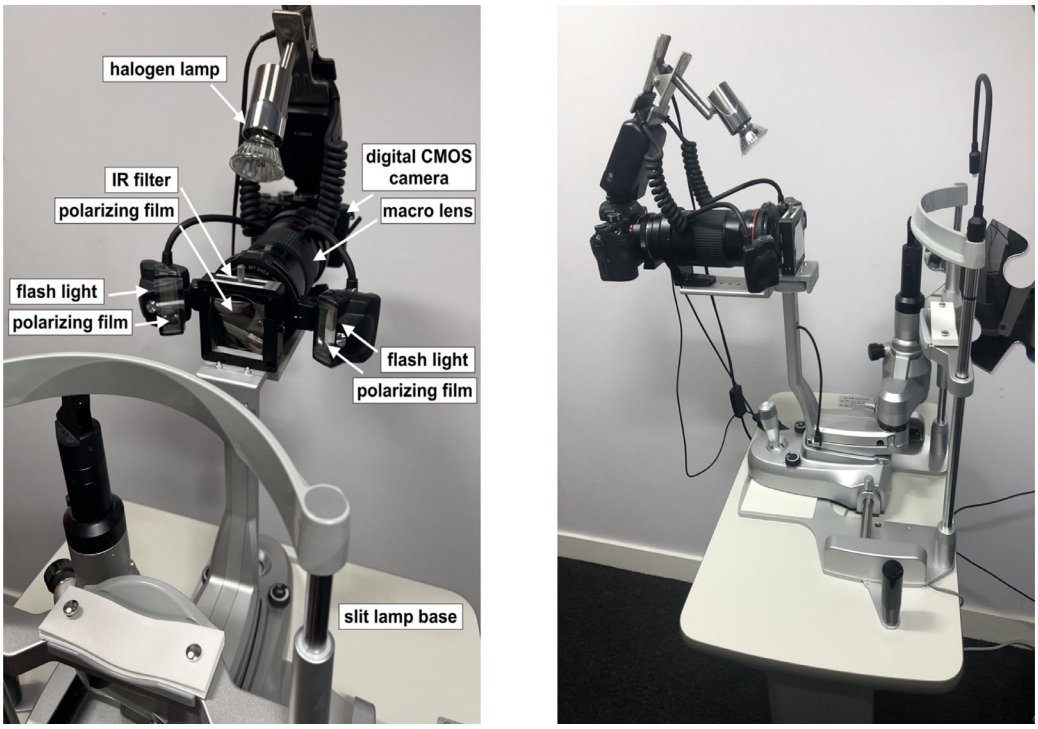

Figure 3. Custom imaging setup used for meibography.

or systemic disorders that would likely affect study outcomes, had a history of corneal refractive surgery, cataract surgery, demonstrated grade 3 or greater in biomicroscopy findings on the Efron Grading Scales, or had another ocular abnormality including Meibomian gland dysfunction or blepharitis, used topical ophthalmic medications, or had significant Meibomian gland dropout that would, in the opinion of the investigator, limit the measurement of gland contrast. Pregnant or breastfeeding women were also excluded. Contact lens wear was not a contraindication for participation in the study, but participants were asked to attend the study visit having not worn their habitual contact lenses or eye makeup that day.

Clinical Assessment

High-contrast, distance logarithm of the minimum angle of resolution visual acuity and slit lamp biomicroscopy of the ocular surface was carried out at the beginning (without fluorescein) and end (with fluorescein) of each visit. Clinical changes to ocular tissues were graded to the nearest 0.1 unit using Efron grading scales. Conjunctival redness, limbal redness, corneal neovascularization, corneal edema, blepharitis, and Meibomian gland dysfunction were assessed at the initial slit lamp examination; additionally, corneal and conjunctival staining and papillary conjunctivitis were assessed after fluorescein instillation. Meibomian gland imaging was performed using a custom imaging setup described elsewhere in this article. Photographs were captured over a range of camera settings and using a number of IR imaging filters in random order (ranging from 600 nm to 1000 nm in 50-nm steps). A total of 90 images were captured for each participant; that is, 9 wavelengths at 10 different ISO settings (from underexposure to overexposure). Ten images were captured during each 1-minute eyelid eversion. There was approximately a 3-minute time interval between eyelid eversions. All procedures were performed by the same examiner (K.S.). The images were further processed using image analysis software to calculate Meibomian gland contrast.

Imaging Setup

The experimental setup is shown in Figure 3. The images were captured with Sony Alpha 7R, 36.3 megapixel full-frame CMOS sensor mirrorless camera (Sony Ltd., Japan), equipped with Canon EF 180-mm f/3.5L USM macro lens (Canon Inc, Tokyo, Japan) and a Canon Macro Twin Lite MT24EX flash (Canon Inc) was used as the light source. The camera sensor was modified by removal of the inbuilt IR filter and replaced with a full spectrum quartz optical

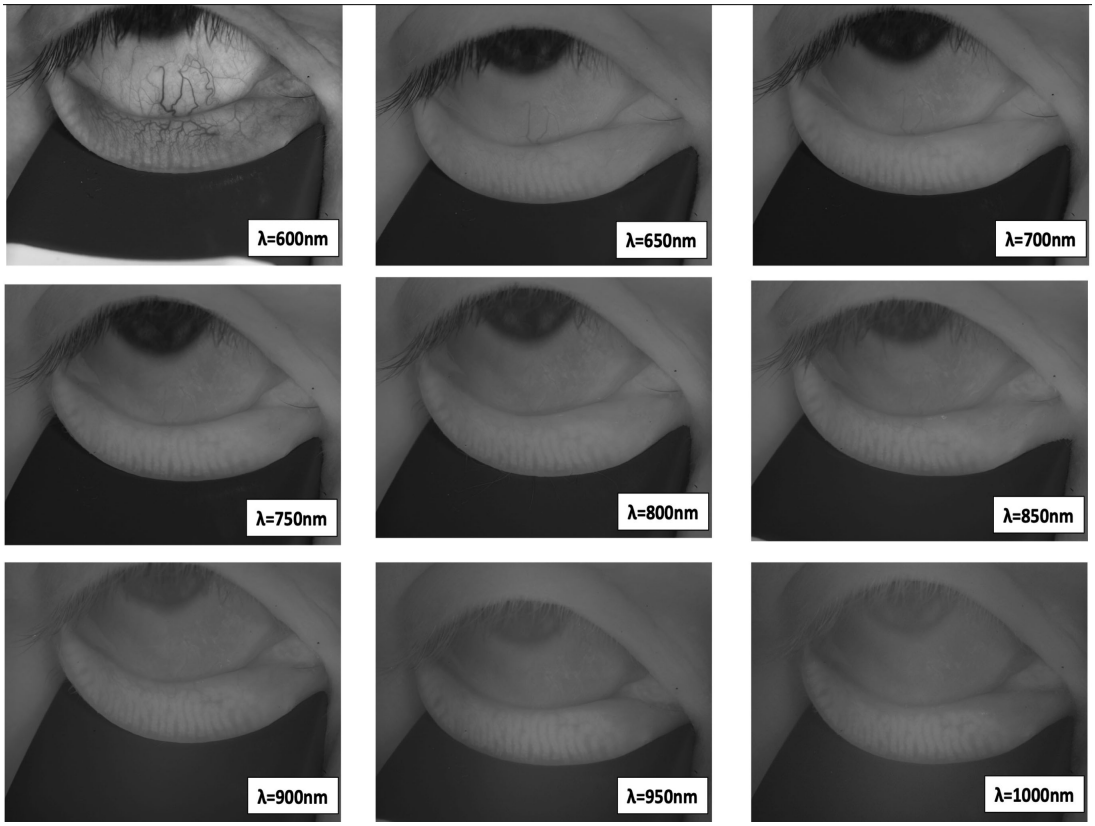

Figure 4. Montage of corrected images for each wavelength captured with new imaging setup for one participant.

element to improve the IR sensitivity of the camera (Advanced Camera Services Ld., Watton, UK). IR filters were mounted directly in front of the lens objective using a 60 mm Cage Plate with Removable Filter Holder (Thorlabs Inc., Newton, NJ, USA). A total of nine TECHSPEC High Performance Shortpass Filters (Edmund Optics Ltd., York, UK) with a 50-mm diameter and a rejection band optical density of 4.0 were used in the study (cut-off wavelength range: 600 nm to 1000 nm in 50-nm steps). TECHSPEC 50 × 50 mm Wire Grid Polarizing Films (Edmund Optics Ltd.) perpendicular to each other were placed in front of lens objective/IR filter and flash lights. All images were captured with an aperture setting of f/18 to get optimal depth of field, that is, to obtain an in-focus image of the entire curved eyelid. A halogen lamp mounted on the top of flash body was used to focus images before the capture. The whole imaging setup was mounted on Takagi 4ZL Slit Lamp base (Takagi Ophthalmic Instruments Europe Ltd., Manchester, UK). Raw images were exported and then converted to gray lossless TIFF files. In total 1350 images were captured. The Handheld Near IR Lid Everter (Johnson & Johnson Vision) was used to facilitate eyelid eversion.

Contrast Calculation

For each wavelength, 10 images for different ISO settings were taken (from underexposed to overexposed). From those images, only one was selected for each wavelength. The image with a mean greyscale level (within the eyelid/gland region as seen in Figure 5b) closest to 127 (a 50% gray level) was selected and then multiplied by a correcting factor to make it exactly 127. Therefore, the exposure was maintained constant across all wavelengths. Region of interest labels were selected manually using the interactive Image Labeler app provided within MATLAB R2022a (The MathWorks, Inc., Natick, MA, USA). The Smart Polygon tool was used to estimate the shape of an object of interest within a drawn polygon. The Smart Polygon tool identifies an object of interest by using regional graph-based segmentation (GrabCut).[12] Estimated regions of interest were further corrected using the Brush tool to make sure that gland labels were defined as precisely as possible. Six central glands were selected for each participant, all images were labelled by one annotator (K.S.), who ensured that the same glands were selected across all wavelengths for each participant. Eyelid masks were limited to half gland

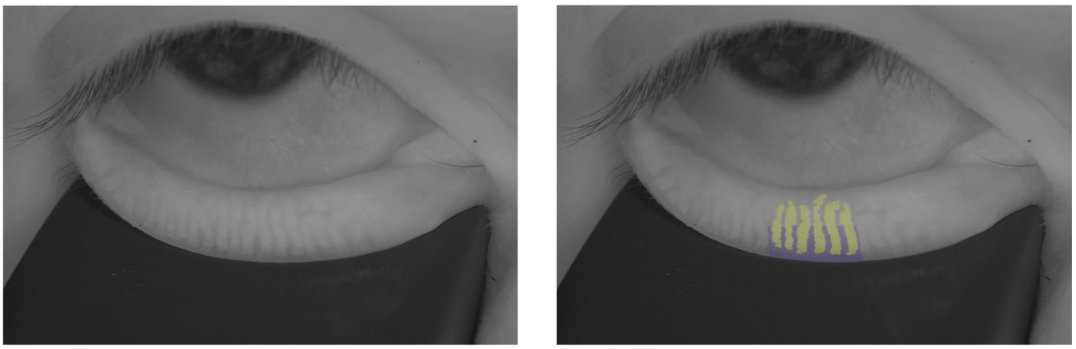

(a) The meibography image of representative participant

(b) Manual annotations of eyelid (blue) and the Meibomian glands (yellow)

Figure 5. Region selection for Meibomian gland contrast calculation. For each participant six central glands were selected (same across all wavelengths).

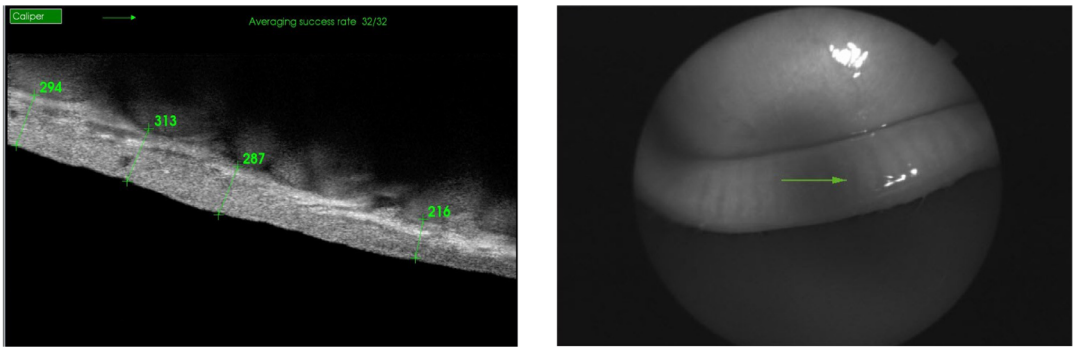

(a) (b)

Figure 6. Meibomian gland depth measurement. A single horizontal scan (green arrow in [b]) was taken for each eyelid with Topcon OCT-2000. Meibomian gland depth was measured as a distance from first tissue margin to each valley seen in the image (green lines in [a]).

height as the upper part of the everted eyelid was much brighter than the lower end and, in some cases, it was difficult to judge whether pixels belonged to the gland or not.

Meibomian gland contrast has been defined as the difference between mean gland region pixel intensity, I_{glands} (range, 0–255; yellow mask in Fig. 5b) and mean eyelid region pixel intensity, I_{eyelid} (blue mask in Fig. 5b). For the purpose of this work, we refer to this as simple contrast (C_{Simple}). It is expressed as:

$$C_{Simple} = I_{glands} - I_{eyelid} \tag{1}$$

The modified Michelson contrast was also calculated to allow direct comparison with other published results on a similar topic and to confirm that our results do not depend on the contrast definition and measurement technique. The altered Michelson contrast has been defined as follows:

$$C_{Michelson} = \frac{I_{glands} - I_{eyelid}}{I_{glands} + I_{eyelid}}, \tag{2}$$

where I_{glands} and I_{eyelid} correspond with the mean gland and eyelid region of interest pixel intensities, respectively.

Meibomian Gland Depth Measurement

A Topcon OCT 2000 anterior segment optical coherence tomography (OCT) device with a swept-source laser wavelength of 840 nm and scanning depth of 2.3 mm (Topcon, Tokyo, Japan) was used to perform a single horizontal 3-mm line scan across the everted lower eyelid of the right eye (Fig. 6b). The lower eyelid was everted with the handheld near IR lid everter (to facilitate eversion only and not

as a light source) for consistency. Meibomian gland depth was measured as the distance from the tarsal conjunctival surface to each peak observed in the image which appears to relate to the Meibomian gland structure (Fig. 6a). The number of glands observed in the image varied across individuals from two to five, with the mean depth for each participant used for further analysis. Meibomian gland depth ranged from 187 µm to 359 µm. Meibomian gland depth assessment is not a standard measurement captured with an OCT and thus the determination of the apparent Meibomian gland position depended on subjective assessment of the examiner. The images were analyzed manually by one observer (K.S.) using the measure caliber tool for distance measurement in the OCT device.

Statistical Analysis

Statistical analysis was performed using MATLAB R2022a with Statistics and Machine Learning Toolbox (The MathWorks, Inc.) and R[13] using the lmerTest package.[14] Meibomian gland image contrast was assessed using a linear mixed model, with filter wavelength as a fixed factor and participant as a random factor. The least square means and their differences were estimated along with confidence intervals and *P* values. Post hoc multiple comparison testing was performed using the Tukey honest significant differences test. The correlation between Meibomian gland contrast and Meibomian gland depth was investigated with Spearman's rank correlation coefficient. Statistical significance was defined as a *P* value of less than 0.05.

Results

Demographics

A total of 15 participants (10 females and 5 males) were included in the study. Only the lower eyelids of the right eye were included. The mean age of study participants was 40.7 ± 10.9 years, ranging from 24 to 58 years. Five participants were contact lens wearers.

Best Wavelength for Optimal Meibomian Gland Contrast

Figure 7 shows Meibomian gland contrast as a function of wavelength for both the simple and Michelson contrasts. The results of the overall linear regression model showed a significant effect of wavelength on Meibomian gland contrast (simple contrast: $F = 7.24$, $P < 0.0001$; Michelson contrast: $F = 7.19$, $P < 0.0001$). A post hoc analysis using the Tukey honest significant differences test showed that the 750-nm wavelength resulted in significantly higher Simple and Michelson contrast than that measured at 650 nm, 900 nm, 950 nm, and 1000 nm. Post hoc analyses also demonstrated that the 1000-nm wavelength showed significantly lower Simple and Michelson contrast in comparison with the 600-nm, 700-nm, 750-nm, 800-nm, and 850-nm wavelengths. The 700-nm wavelength has also statistically greater simple and Michelson contrast, in comparison with the 650-nm and 950-nm wavelengths. These comparisons are presented in Tables 1 and 2. Table 3 shows the percentage of patients for who

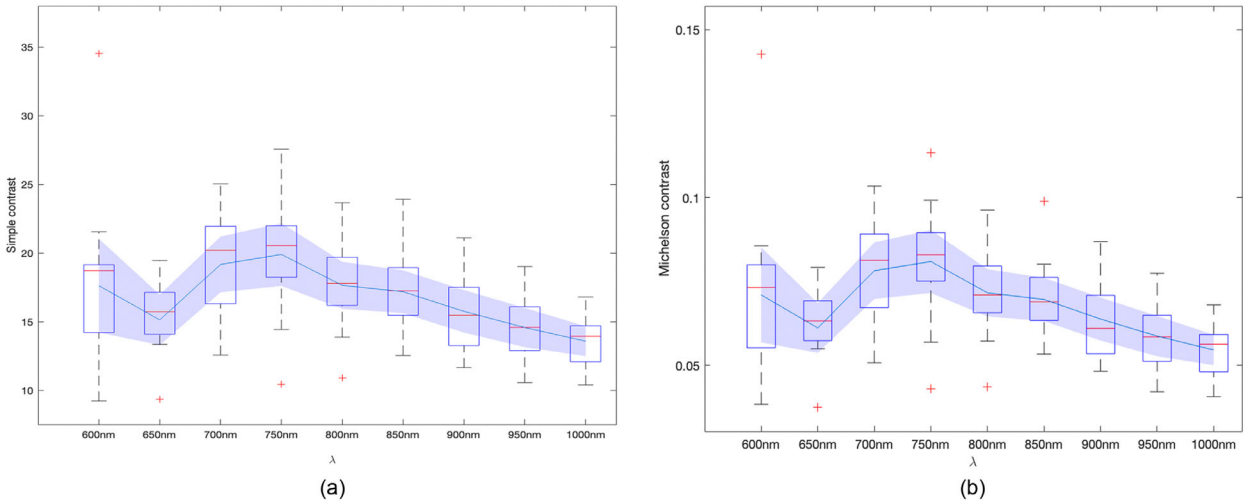

Figure 7. Simple contrast (a) and Michelson contrast (b) as a function of wavelength. The blue line shows the mean and the filled polygonal regions around the mean show its 95% confidence intervals.

Table 1. Multiple Comparisons Tukey's Honest Significant Difference Test Results for Simple Contrast for Selected Wavelengths

Wavelength (I)	Wavelength (J)	Mean Difference (I–J)	Lower CL	Upper CL	*P* Value
1000	600	−4.04	−7.56	−0.52	0.0121
	700	−5.59	−9.11	−2.07	0.0001
	750	−6.31	−9.83	−2.79	<0.0001
	800	−4.07	−7.59	−0.55	0.0113
	850	−3.60	−7.12	−0.08	0.0405
700	650	4.04	0.52	7.56	0.0125
	950	4.59	1.07	8.11	0.0022
750	650	4.76	1.24	8.28	0.0013
	900	4.13	0.61	7.65	0.0093
	950	5.32	1.80	8.84	0.0002
	1000	6.31	2.79	9.83	<0.0001

Only statistically significant comparisons are presented.

Table 2. Multiple Comparisons Tukey's Honest Significant Difference Test Results for Michelson Contrast for Selected Wavelengths

Wavelength (I)	Wavelength (J)	Mean Difference (I–J)	Lower CL	Upper CL	*P* Value
1000	600	−0.0164	−0.0312	−0.0017	0.0176
	700	−0.0237	−0.0384	−0.0089	0.0001
	750	−0.0264	−0.0412	−0.0116	<0.0001
	800	−0.0171	−0.0318	−0.0023	0.0115
	850	−0.0151	−0.0299	−0.0003	0.0416
700	650	0.0171	0.0023	0.0319	0.0011
	950	0.0195	0.0047	0.0343	0.0019
750	650	0.0198	0.0050	0.0346	0.0015
	900	0.0171	0.0024	0.0319	0.0108
	950	0.0222	0.0075	0.0370	0.0002
	1000	0.0264	0.0116	0.0412	<0.0001

Only statistically significant comparisons are presented.

Table 3. Distribution of Patients Across Different Wavelengths

	Wavelength (nm)								
	600	650	700	750	800	850	900	950	1000
% of patients for who both simple and Michelson contrast were greatest	6.7	6.7	40.0	26.7	0.0	20.0	0.0	0.0	0.0
% of patients for who both simple and Michelson contrast were lowest	20.0	13.5	0.0	0.0	6.7	6.7	6.7	13.3	33.3

contrast was the greatest and the lowest for particular wavelength.

Correlation Between Meibomian Gland Depth and Meibomian Gland Contrast

There was a significant negative correlation between Meibomian gland contrast and Meibomian gland depth for the 750-nm IR filter. This was observed for both Simple and Michelson contrast. The results are shown in Table 4 and Figure 8.

Discussion

In this work, we introduced a custom imaging system that has been developed to provide high-

Table 4. Spearman's Rank Correlation Coefficients (ρ_s) and *P* Values for Each Wavelength for Both Simple and Michelson Contrasts

	Meibomian Gland Depth ρ_s	*P* Value
Simple contrast		
600 nm	−0.439	0.103
650 nm	−0.286	0.301
700 nm	−0.314	0.254
750 nm	−0.579	0.026
800 nm	−0.304	0.271
850 nm	0.200	0.474
900 nm	−0.293	0.289
950 nm	0.004	0.995
1000 nm	−0.129	0.648
Michelson contrast		
600 nm	−0.346	0.206
650 nm	−0.275	0.320
700 nm	−0.375	0.169
750 nm	−0.579	0.026
800 nm	−0.286	0.301
850 nm	0.321	0.242
900 nm	−0.268	0.333
950 nm	−0.014	0.964
1000 nm	−0.129	0.648

resolution, wide depth-of-field, reflection-free, multispectral IR imaging of the Meibomian glands. Our results demonstrate that IR filter of 750 nm is the optimal choice for Meibomian gland imaging because it typically provides images of greatest contrast. Both simple and Michelson contrasts for this wavelength are significantly greater than for other wavelengths (650 nm, 900 nm, 950 nm, and 1000 nm). The wavelength of 1000 nm seems to give the worst contrast results as the values for this wavelength are significantly lower than for other wavelengths, this includes the wavelength of 600 nm, 700 nm, 750 nm, 800 nm, and 850 nm. Furthermore, Meibomian gland contrast (both simple and Michelson) for the wavelength of 750 nm negatively correlates with Meibomian gland depth meaning that glands that are deeper into tarsal plate appear more faded in meibography. Possible reasons for this include an increase in light scatter deeper in the tissue, causing lower contrast. Further investigation may identify imaging enhancements to compensate for or overcome this issue. In addition, as mentioned elsewhere in this article, Meibomian gland depth assessment is not a standard measurement captured with an OCT and is not well-described in the literature; thus, the determination of the apparent Meibomian gland position depended on the subjective assessment of the examiner. This possible correlation requires further investigation in a properly sampled population with different instruments to confirm our findings. Although the wavelength of 750 nm is the optimal choice for best Meibomian gland contrast, our study showed that some individuals may benefit from a different wavelength for imaging based on the overall depth of the tissue. Results presented in Table 3 show the wide range of wavelengths that works for different people. Those differences imply that Meibomian gland

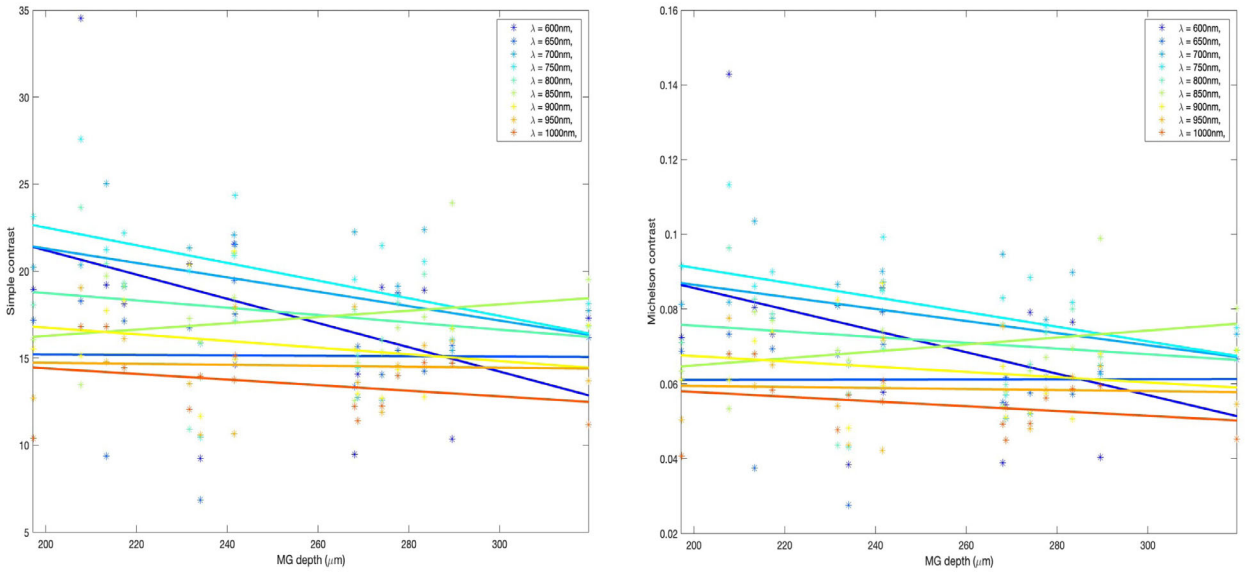

(a) (b)

Figure 8. Correlation between Meibomian gland contrast ([a] Simple contrast, [b] Michelson contrast) and Meibomian gland depth. Each line corresponds with a different wavelength of the IR filter used for imaging.

depth may play an important role in meibography. As such, future imaging designs may include range of different wavelengths to optimize image capture.

However, the findings of the current study do not support the previous research. A similar study by Peral et al.[9] suggests that the greatest contrast of Meibomian glands is obtained for wavelength of 600 nm. The authors designed the experimental setup with tunable monochromatic light outputting IR light from 600 to 1050 nm in 25-nm steps. The reported Michelson contrast values ranged from 0.04 to 0.06, similar to our own work (0.05–0.08). In the aforementioned study, the contrast varied across individuals, as was also observed in our study, resulting in the conclusion that Meibomian gland contrast depends on Meibomian gland depth, as shown in the second part of this study. Even though Peral et al.[9] used a more sophisticated method of pixel selection based on local maxima and minima detection, we believe that the images captured at the 600-nm wavelength may provide false results, because other than glands structures become more apparent, such as blood vessels (as seen in Fig. 4), which seem to be much darker than the actual intergland region; as such, they may contribute to the overall contrast value calculated with Peral et al.[9] method. The authors have reported that the second wavelength that gave the greatest contrast was 775 nm, which would align with the result of the current study.

Keratograph 5M operates at wavelength of 840 nm and LipiView II in an IR spectrum between 890 and 940 nm.[15] This study highlighted that contrast tends to decrease after reaching a peak at 750 nm. This outcome is contrary to that of Peral et al.,[9] who found that Meibomian gland contrast (both simple and Michelson) tends to increase above the 900-nm wavelength. The apparent decrease in Meibomian gland contrast with increasing wavelength observed in our study may relate to the decreased sensitivity of the study camera for longer wavelength IR light. As can be seen in Figure 4, hot spots (bright areas in the center of the frame) become more apparent for longer wavelengths. Also, hot spots are worse at smaller apertures (larger f numbers), as in our setup. It is possible that the cameras used in commercially available devices have better IR sensitivity and/or IR optics allow them to operate effectively over longer wavelengths.

This experiment provides a new insight into the relationship between Meibomian gland contrast (measured with two different methods) and Meibomian gland depth. Specifically, the current study provides tentative initial evidence that Meibomian gland contrast depends on Meibomian gland depth. These results should be taken into account when imaging Meibomian glands, because glands that are situated deeper into the tarsal plate typically seem to be dimmer on IR photography. Our results show also that those glands may require a longer wavelength for imaging to obtain better contrast. In Figure 8, a shift in imaging wavelength for deeper situated glands can be seen. This observation is most apparent for the 600-nm wavelength (navy blue line), which gives optimal contrast for shallower glands but much worse for deeper glands. In reviewing the literature, no data were found on the association between Meibomian gland depth and Meibomian gland contrast. To our knowledge, this study is the first to investigate this relationship.

Meibomian gland intensity metrics (metrics based on grayscale level of the image) have been successfully used to track changes of the Meibomian glands.[4,9–11] Yeh and Lin[16] have reported that Meibomian gland contrast (defined as an average difference between the mean intensity along the Meibomian glands and the mean intensity along the regions between the glands, which corresponds with the simple contrast in our study) may be a good diagnostic test for the diagnosis of lipid-deficient dry eye because patients with lipid-deficient dry eye have a significantly lower contrast than controls.[16] Although our study did not investigate the difference between groups, it has shown a high variability in contrast for each wavelength and each participant. The same group have also determined repeatability and limits of agreement of Meibomian gland contrast for Keratograph 5M.[4] It has been shown that contrast changes (in grayscale, 0–255) greater than 11 units in the upper eyelid or 18 units in the lower eyelid are more likely caused by physiological changes rather than the head position or room lighting.[4] Because the flash is much more powerful than the continuous light and has broader IR spectral distribution than typical room lightning, images were independent on ambient lighting in our study. Moreover, the handheld eyelid everter that was adopted to assist in eyelid eversion, provided consistent eyelid eversion across various wavelengths.

A number of studies have proposed and evaluated various Meibomian gland intensity metrics, other than contrast, such as the gland signal index, mean, standard deviation, median, mode, energy, relative energy, entropy, standard deviation irregularity of the selected pixels, kurtosis, and skewness of region of interest histograms.[17,18] It has been shown that those metrics could be a promising biomarker for Meibomian gland dysfunction because patients with a higher level of dropout had significantly lower visibility.[17,18] It has been also shown that those visibility metrics correlate with bulbar redness, tear meniscus height, meibum expressibility score, and noninvasive

tear break-up time.[11] Furthermore, it has been proposed that median pixel intensity in combination with ocular surface metrics such as, dropout percentage, tear meniscus height, lid margin abnormality score, and Ocular Surface Disease Index score can be a powerful tool for a Meibomian gland dysfunction diagnosis.[11] Once again, analyses of those studies was based on images obtained with a Keratograph 5M. In our study, we focus on the measurement of contrast, but the image analysis could be easily extended to more parameters. Nonetheless, it is worth highlighting that Meibomian gland reflectivity measurement is of great interest to many researchers and is of significant importance for Meibomian gland health assessment.

Although the study has demonstrated successfully that Meibomian gland contrast varies across individuals and is influenced by Meibomian gland depth, it has certain limitations. The relatively small sample size represents the exploratory nature of this study. Another source of uncertainty is the possibility of measurement errors in manual annotations of Meibomian gland images. Even though the images were labelled by one annotator, it is still a subjective matter to decide whether pixels in the image belong to gland or eyelid region. A more reliable, repeatable, objective method of meibography image segmentation is needed. There are a number of examples in the literature that implement artificial intelligence–based algorithms to perform this task objectively in repeatable and reliable way.[19–25] However, those type of tasks depend on the image type analyzed and the device they have been captured with; as such, it is our future goal to develop an objective method that would be suitable for images captured with the system presented in this work. Another limitation of the current study is that Meibomian gland depth measurements were based on the examiner's judgment of the location of Meibomian glands. A limited number of studies have used OCT to measure depth of Meibomian glands, with little evidence on the measurement of such features with the device.[26,27] Despite its limitations, the study certainly adds to our understanding of the Meibomian gland imaging. Several questions still remain to be answered. A natural progression of this work is to run a larger clinical trial to determine the diagnostic capability of Meibomian gland contrast measured with this newly developed system. More broadly, research is also needed to confirm the Meibomian gland depth measurement with OCT. A further study could also assess Meibomian gland contrast of the upper eyelid glands because they have slightly different morphological characteristics, and it is possible that contrast could differ as well.

An implication of these findings is that both imaging wavelength and Meibomian gland depth should be taken into account when measuring Meibomian gland contrast. Because meibography has been used widely in optometry practice, it is important to better understand its strengths and weaknesses. Many commercially available devices provide processed images, which are good for the subjective analysis of Meibomian gland health. However, image processing often compromises contrast measurement. Thus, we have proposed a new system that is optimized for the assessment of intensity-based Meibomian gland metrics.

Acknowledgments

The authors thank their clinical, logistical, and administrative colleagues at Eurolens Research for their assistance in the acquisition of data for this study.

Disclosure: **K. Swiderska**, None; **C.A. Blackie**, Johnson & Johnson Vision, Inc (E); **C. Maldonado-Codina**, None; **M. Fergie**, None; **P.B. Morgan**, None; **M.L. Read**, None

References

1. Arita R. Meibography: A Japanese perspective. *Invest Ophthalmol Vis Sci*. 2018;59(14):DES48–DES55.
2. Jester JV, Rife L, Nii D, Luttrull JK, Wilson L, Smith RE. In vivo biomicroscopy and photography of meibomian glands in a rabbit model of meibomian gland dysfunction. *Invest Ophthalmol Vis Sci*. 1982;22(5):660–667.
3. Hwang HS, Xie Y, Koudouna E, Na KS, Yoo YS, Yang SW, et al. Light transmission/absorption characteristics of the meibomian gland. *Ocular Surf*. 2018;16(4):448–453.
4. Yeh TN, Lin MC. Repeatability of Meibomian gland contrast, a potential indicator of Meibomian gland function. *Cornea*. 2019;38(2):256–261.
5. Zouboulis CC. Isotretinoin revisited: Pluripotent effects on human sebaceous gland cells. *J Invest Dermatol*. 2006;126(10):2154–2156.
6. Nelson AM, Gilliland KL, Cong Z, Thiboutot DM. 13-cis Retinoic acid induces apoptosis and cell cycle arrest in human SEB-1 sebocytes. *J Invest Dermatol*. 2006;126(10):2178–2189.
7. Tanriverdi C, Tabakci BN, Donmez S. Longitudinal assessment of meibomian glands and tear film

layer in systemic isotretinoin treatment. *Eur J Ophthalmol*. 2021;20:11206721211018361.
8. Singh S, Naidu GC, Vemuganti G, Basu S. Morphological variants of meibomian glands: Correlation of meibography features with histopathology findings. *Br J Ophthalmol*. 2021;107(2):195–200.Epub Ahead of Print.
9. Peral A, Alonso J, Gomez-Pedrero JA. Effect of illuminating wavelength on the contrast of meibography images. *OSA Contin*. 2018;1(3):1041–1054.
10. García-Marqués JV, García-Lázaro S, Martínez-Albert N, Cervinõ A. Meibomian glands visibility assessment through a new quantitative method. *Graefes Arch Clin Exp Ophthalmol*. 2021;259(5):1323–1331.
11. García-Marques JV, García-Lázaro S, Talens-Estarelles C, MartínezAlbert N, Cervinõ A. Diagnostic capability of a new objective method to assess Meibomian gland visibility. *Optometry Vision Sci*. 2021;98(3):1045–1055.
12. Rother C, Kolmogorov V, Blake A. Grabcut: Interactive foreground extraction using iterated graph cuts. *ACM Transactions on Graphics (SIGGRAPH)*. 2004;23:309–314;
13. R Core Team. *R: A language and environment for statistical computing*. Vienna, Austria: R Foundation for Statistical Computing; 2017, https://www.R-project.org/.
14. Kuznetsova A, Brockhoff PB, Christensen RHB. lmerTest package: Tests in linear mixed effects models. *J Stat Softw*. 2017;82(13):1–26.
15. Grenon SM, Korb DR, Grenon J, Liddle S, Bacich S. Eyelid illumination systems and methods for imaging meibomian glands for meibomian gland analysis. TearScience Inc. 2014. US patent 2014/0330129 A1, https://patents.google.com/patent/US20140330129A1/en.
16. Yeh TN, Lin MC. Meibomian gland contrast sensitivity and specificity in the diagnosis of lipid-deficient dry eye: A pilot study. *Optom Vis Sci*. 2021;98(2):121–126.
17. Deng Y, Wang Q, Luo Z, Li S, Wang B, Zhong J, et al. Quantitative analysis of morphological and functional features in Meibography for Meibomian gland dysfunction: Diagnosis and grading. *EClinicalMedicine*. 2021;40:101132.
18. Xiao P, Luo Z, Deng Y, Wang G, Yuan J. An automated and multiparametric algorithm for objective analysis of meibography images. *Quant Imaging Med Surg*. 2020;11(4):1586599–1586615.
19. Wang J, Yeh TN, Chakraborty R, Yu SX, Lin MC. A Deep learning approach for meibomian gland atrophy evaluation in meibography images. *Transl Vis Sci Technol*. 2019;8(6):37.
20. Setu MAK, Horstmann J, Stern ME, Steven P. Automated analysis of meibography images: Comparison between intensity, region growing and deep learning-based methods (abstract). *Ophthalmologe*. 2019;116(Suppl 2).
21. Prabhu SM, Chakiat A, S S, Vunnava KP, Shetty R. Deep learning segmentation and quantification of Meibomian glands. *Biomed Signal Process Control*. 2020;57:101776.
22. Yeh CH, Yu SX, Lin MC. Meibography phenotyping and classification from unsupervised discriminative feature learning. *Transl Vis Sci Technol*. 2021;10(2):4.
23. Setu MAK, Horstmann J, Schmidt S, Stern ME, Steven P. Deep learning based automatic meibomian gland segmentation and morphology assessment in infrared meibography. *Sci Rep-Uk*. 2021;11(1):7649.
24. Khan ZK, Umar AI, Shirazi SH, Rasheed A, Qadir A, Gul S. Image based analysis of meibomian gland dysfunction using conditional generative adversarial neural network. *BMJ Open Ophthalmol*. 2021;6(1):e000436.
25. Wang J, Li S, Yeh TN, Chakraborty R, Graham AD, Yu SX, et al. Quantifying Meibomian gland morphology using artificial intelligence. *Optometry Vision Sci*. 2021;98(9):1094–1103.
26. Liang Q, Pan Z, Zhou M, Zhang Y, Wang N, Li B, et al. Evaluation of optical coherence tomography meibography in patients with obstructive Meibomian gland dysfunction. *Cornea*. 2015;34(10):1193–1209.
27. Cui X, Wu Q, Zhai Z, Yang Y, Wei A, Xu J, et al. Comparison of the Meibomian gland openings by optical coherence tomography in obstructive Meibomian gland dysfunction and normal patients. *Journal of Clinical Medicine*. 2020;9(10):3181.